Continuous and discontinuous shear thickening in granular suspensions

Abdoulaye Fall, Anael Lemaitre, François Bertrand, Daniel Bonn, Guillaume Ovarlez

HAL Id: hal-00490742

https://hal.archives-ouvertes.fr/hal-00490742v1

Submitted on 9 Jun 2010 (v1), last revised 2 May 2011 (v2)

Continuous and discontinuous shear thickening in granular suspensions

Abdoulaye Fall[1,2], Anaël Lemaître[1], François Bertrand[1], Daniel Bonn[2,3], Guillaume Ovarlez[1]

[1] *Université Paris Est, Laboratoire Navier (CNRS UMR 8205), 2 allée Kepler, 77420 Champs sur Marne, France*
[2] *Van der Waals-Zeeman Institute, University of Amsterdam, Valckenierstraat 65, 1018XE Amsterdam, The Netherland*
[3] *Laboratoire de Physique Statistique, Ecole Normale Supérieure, 24 Rue Lhomond, 75005 Paris, France*

We study the emergence of shear thickening in dense suspensions of non-Brownian particles. We combine local velocity and concentration measurements using Magnetic Resonance Imaging with global rheometric experiments. We evidence a continuous transition at very low shear rate from a viscous to a shear thickening, granular, rheology characterized by shear stresses proportional to the shear rate squared. We show that an unexpectedly fast migration of grains occurs towards low shear zones as a result of the granular rheology. Combining local and global measurements allow to show that the interplay between flow and migration is responsible for the macroscopic observation of discontinuous shear thickening, but that locally the shear thickening is continuous.

The realm of complex fluids encompasses biological liquids such as blood, many liquid foodstuffs, building materials, glasses and plastics, crude oil, etc. Despite their importance, the most basic, quintessential question about the flow of these fluids has remained unanswered: it is generally impossible to predict their flow resistance, and it is even unclear why most fluids shear thin, whereas only some shear thicken. Understanding shear thickening, i.e. the increase of the apparent viscosity of materials with increasing flow rate, is thus an important issue in complex fluids with in addition a strong impact on energy consumption in industrial processes [1]. It is observed in dense colloidal suspensions [1,2], where it has been related to the formation of dense clusters of particles [2-4]. The viscosity rise with the shear rate is then usually reversible (it is a steady-state property), continuous, and is sharper at higher volume fractions [2-4]. For colloids, the competition between shear-induced cluster formation and Brownian motion that homogenizes the suspensions then naturally determine a critical shear rate for the onset of shear thickening.

As Brownian motion is absent in pastes made of large particles, the sharp shear thickening transition observed in for instance cornstarch suspensions [5] is highly surprising. In fact, the conditions of emergence of shear thickening in non-Brownian suspensions remain ill-characterized: in some systems, thickening was observed at low shear rates [1,5-7], while in others no shear thickening (only viscous behavior) is observed whatsoever, even close to jamming [8-10]. Up to now it is thus impossible to predict whether a given system will shear thicken or not.

In systems for which it is observed, a more pronounced shear thickening [6,7] is observed near jamming, similarly to colloidal suspensions, and is attributed to aggregation of hydroclusters into a percolating network [4,11]. Brown and Jaeger [7] thus suggest that discontinuous shear thickening is a limiting behavior approached at the jamming packing fraction. However, one should question whether these observations of discontinuous shear thickening reflect an intrinsic (local, steady-state) property of materials. For example, an important effect of confinement on shear thickening was recently evidenced in both colloidal [12] and noncolloidal [5] suspensions. In channel flows [12], the macroscopic shear thickened state was shown to form a plug flow and was not observed in large channels, which show that local observations are crucial to get a better insight into shear thickening.

In this Letter, we address these puzzles by studying the emergence of shear thickening in the simplest of systems: model density-matched suspensions of particles in water. We use a wide gap Couette geometry to avoid confinement effects, and we access the intrinsic material behavior by measuring the local flow properties and particle concentration using Magnetic Resonance Imaging (MRI). We show that the *local* rheology presents a *continuous* transition, from a viscous to a shear thickening, granular, behavior. In the second, granular, regime we find an unexpectedly fast migration of grains towards the low shear zones, which we explain as a direct consequence of the shear thickening behavior. These observations, when combined, allow us to show that the interplay between flow and migration is responsible for the *macroscopic* observation of *discontinuous* shear thickening, which is thus not an intrinsic property of granular suspensions. The critical shear rate for thickening then emerges as a consequence of the existence of the two flow regimes.

Materials and methods — We study dense suspensions of noncolloidal monodisperse spherical particles immersed in a Newtonian fluid. We use polystyrene beads (diameter $40\mu m$, polydispersity <5%, density $1.05 g.cm^{-3}$) suspended in aqueous solutions of *NaI* to match the solvent and particle densities; the solution viscosity is 1mPas. The density matching ensures that there are no gravity-induced contacts [13] and that the only source of normal stresses is shear [14,15]. We focus on results obtained at a 59% mean volume fraction as experiments at other high volume fractions show similar features. The material behavior is studied with a wide-gap Couette rheometer (inner radius: 4.1*cm*; outer radius: 6*cm*; height of sheared fluid: 11*cm*) inserted in a MRI scanner, allowing us to

access local velocity and particle volume fraction profiles in the flowing sample [9,16,17]. Sandpaper is glued to the walls and there is no significant slip on the velocity profiles. The inner cylinder velocity is controlled, and we record the torque exerted by the material on the inner cylinder with a Bohlin rheometer.

Macroscopic vs. local behavior — We first focus on the macroscopic behavior (Fig. 1a). The torque T values measured during a slow ramp in rotational velocity Ω are shown as black circles. At the beginning of the ramp, T increases linearly with Ω, as expected for a homogeneous, Newtonian suspension [9,10]. Around $\Omega_c \approx$ 2.5 rpm (corresponding to a low average shear rate of $0.6s^{-1}$), T presents a sudden increase – by a factor of 20 – which is a clear signature of "discontinuous" shear thickening, following which T continues to increase with Ω, yet at a slower pace. The above behavior is similar to that observed in [7] in dense suspensions of glass beads. At the end of the ramp, Ω is kept constant and T reaches a stationary value. Subsequent slow changes (down or up) of the rotational velocity then drive the system reversibly along the curve $T(\Omega)$ in open symbols, i.e. the system has reached steady state. This curve presents very smooth, moderate, "continuous" shear thickening.
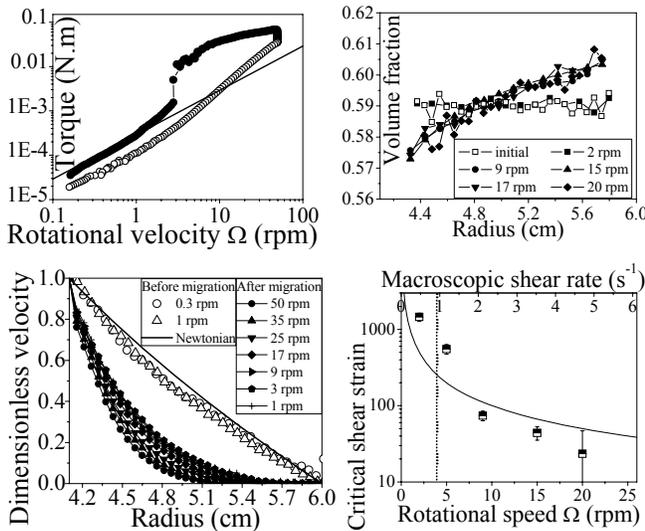

Fig. 1: a) Torque vs. rotational velocity Ω when shearing a 59% suspension: increasing velocity ramp (filled circles) and stationary state (empty circles); the line is a viscous law. b) Volume fraction vs. radius R, for various Ω, during an increasing velocity ramp. c) Dimensionless velocity vs. R (empty symbols: before migration, filled symbols: various Ω after migration, line: Newtonian velocity profile). d) Critical strain needed to complete migration in a 59% suspension vs. Ω; the dotted line indicates the $\dot\gamma / \dot\gamma^2$ transition on the 59% suspension. The line is a $1/\dot\gamma$ scaling.

During the initial increasing velocity ramp, at a low rotational velocity, Ω=2 rpm ($<\Omega_c$), the density $\phi(R)$ remains uniform (Fig. 1b) while the flow (Fig. 1c) is

homogeneous– there is no jammed region [5]. The velocity profile $V(R)$ closely matches that of a Newtonian fluid (Fig. 1c) [9,18], consistent with the initial linear behavior of the torque. Shortly after shear thickening occurs (here at Ω=9 rpm) we observe that the material has become strongly heterogeneous (Fig. 1b) while the velocity profiles present a jammed region near the outer cylinder. This change is irreversible: the density profiles subsequently remain similar, even when Ω is increased further and, later, decreased below Ω_c.

Clearly, the discontinuous shear thickening observed during the initial up-ramp is a transient phenomenon associated with a large-scale reorganization of the material, which involves *shear-induced migration* from low to high shear zones. While migration is expected in dense suspensions [9,19-21], it is particularly striking here that the change in $\phi(R)$ occurs over a very short time interval, corresponding to a small total strain of order 100. Such a rapid migration is a puzzle as it is not predicted by classical theories [9].

Constitutive behavior — We now analyze the steady state behavior. We first note that density and velocity profiles are in steady state whenever the torque is. Moreover, while $\phi(R)$ is Ω-independent in steady state, the dimensionless velocity profiles $V(R)/V(R_i)$ do not superpose, implying that the local behavior cannot be simply viscous [9,18]. Finally, the flow is always strictly localized: for all Ω, there is a jammed region beyond a critical radius R_m=5.7cm; this corresponds to density threshold $\phi(R)>\phi_m\approx60.5\%$ above which the material is jammed [9].

The material and flow being heterogeneous, torque measurements $T(\Omega)$ are insufficient to infer the intrinsic constitutive behavior. This can however be done using our local measurements. The key point [9] is that the steady state density profile $\phi(R)$ is independent of Ω; a change of variables can be then performed between radius R and $\phi(R)$. In addition, the stress profile is prescribed by momentum balance $\tau(R) = T/(2\pi HR^2)$ while the local shear rate can be extracted from the velocity profile $V(R)$ via: $\dot\gamma(R) = R\,\mathrm{d}(V/R)/\mathrm{d}R$. A stress/strain-rate curve $\tau(\dot\gamma,\phi)$ – at fixed and well-defined density ϕ – is then obtained by collecting all measurements of local stress $\tau(R)$ and shear rate $\dot\gamma(R)$ for a fixed R and varying Ω.

The results of this analysis (Fig. 2a) show that for a fixed volume fraction, a clear transition from a $\tau \propto \dot\gamma$ (Newtonian) to a $\tau \propto \dot\gamma^2$ (Bagnoldian) regime occurs at a critical shear rate $\dot\gamma_c(\phi)$ (Fig. 2b). The $\dot\gamma^2$ regime is reminiscent of the constant volume fraction behavior of dry granular materials [22,23]. It is the first experimental signature of a "granular rheology" in

dense suspensions. The $\dot{\gamma}^2$ scaling needs not to be associated with collision-dominated flows as Bagnold suggested [24] – a situation which must be ruled out in our highly damped system. It however signals a regime dominated by particle inertia [8,22,23]: how can this arise in our dense, highly damped, suspension, with particles of size ~10μm? To answer this question, we need to better understand the behavior of the critical shear rate for the viscous/granular transition: it is particularly striking that $\dot{\gamma}_c$ (i) is rather low (of order 1s^{-1}), (ii) vanishes almost linearly as the volume fraction tends to $\phi_c \approx 60.5\%$, which (iii) is identical – within the experimental accuracy – to the threshold ϕ_m at which the material jams.
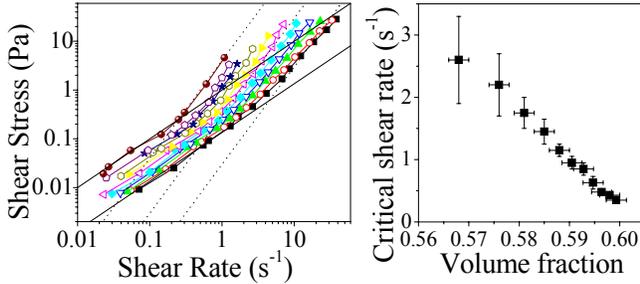

Fig. 2: a) Local shear stress vs. local shear rate measured for various local volume fractions when varying the inner cylinder rotational velocity from 0.1 to 50rpm (from right to left: ϕ=56.8%, 57.6%, 58.1%, 58.5%, 58.8%, 59%, 59.3%, 59.5%, 59.7%, 59.8%, 60%). The full lines are $\dot{\gamma}$ scaling; the dotted line are $\dot{\gamma}^2$ scaling. b) Critical shear rate for the $\dot{\gamma}/\dot{\gamma}^2$ transition vs. volume fraction.

Viscous/inertial transition — To understand what controls these scaling regimes, following [22,23], we write Newton's equations for a set of rigid particles. For the particles' centers of mass r_i these read: $m\, \mathrm{d}^2 r_i/\mathrm{d}t^2 = \sum_j F_{ij} + F_i^{visc}$ where F_{ij} denote rigid contact forces and F_i^{visc} hydrodynamic forces which we suppose linear in terms of all the velocities entering into the problem. No other force is supposed to be involved. The key of the analysis is to remark that if F_{ij} are rigid forces, they do not introduce, by definition, any force or length scale. We then consider the two limiting cases: "viscous" (V) when viscous forces are dominant over grain inertia $0 = \sum_j F_{ij} + F_i^{visc}$, and "inertial" (I) when grain inertia is dominant $m\, \mathrm{d}^2 r_i/\mathrm{d}t^2 = \sum_j F_{ij}$. Both expressions verify exact scale invariance by a change of time and force units [23], guaranteeing $F_{ij} \propto \dot{\gamma}$ in (V) and $F_{ij} \propto \dot{\gamma}^2$ in (I), with identical scaling for all components of the stress tensor. The full problem then reduces to (V) (resp. (I)) at low (resp. high) $\dot{\gamma}$, which explains the existence of a crossover between the two simple scaling regimes $\tau \propto \dot{\gamma}$ (viscous) and $\tau \propto \dot{\gamma}^2$ (inertial).

This formalism now helps us understand why the critical shear rate $\dot{\gamma}_c(\phi)$ is so low and vanishes precisely at ϕ_m. In the viscous (V) and inertial (I) regimes, the stresses read respectively $\tau = \Sigma_V(\phi)\dot{\gamma}$ and $\tau = \Sigma_I(\phi)\dot{\gamma}^2$. Numerical simulations [25] indicate that $\Sigma_I(\phi)$ and $\Sigma_V(\phi)$ should diverge at the same (jamming) packing fraction ϕ_m and read $\Sigma_I(\phi) \sim (\phi_m - \phi)^{-\alpha_I}$, $\Sigma_V(\phi) \sim (\phi_m - \phi)^{-\alpha_V}$. The crossover between the viscous and inertial regimes is found by equating the two expressions for the stress, finally leading to $\dot{\gamma}_c(\phi) \sim (\phi_m - \phi)^{\alpha_I - \alpha_V}$. Together with the values $\alpha_I = 2$, $\alpha_V = 1$ proposed in the literature [26,27], this equation explains: (i) that $\dot{\gamma}_c(\phi)$ vanishes at the jamming packing fraction ϕ_m, as observed, and (ii) that it vanishes linearly with ϕ. Moreover, the crossover stress verifies $\tau_c(\phi) \sim (\phi_m - \phi)^{\alpha_I - 2\alpha_V}$, which suggests that it should be independent of volume fraction. Although our stress measurements are not sufficiently accurate to assert that $\tau_c(\phi) \sim \mathrm{cst}$, we then note in Fig. 2a that, indeed, in the experiments τ_c does not vary much. We finally conclude that it is the difference in singular behavior of the inertial and viscous stresses at the approach of jamming which leads to the linear vanishing of $\dot{\gamma}_c(\phi)$, and hence permits this transition to take place at low strain rates.

Accelerated shear-induced migration — We now show that this transition also explains the sudden migration associated with the macroscopically observed discontinuous shear thickening (Fig. 1a). In viscous suspensions, shear-induced migration is usually thought to be negligible when small particles are involved. The typical strainscale for migration is indeed very large: it is expected to be rate independent and to scale as $\propto (R_o - R_i)^2/a^2$ [9,19-21], leading to an expected strain of order 50000 [9], more than 500 times higher than what we observe here at the onset of shear thickening. Our observations may be understood by considering migration in the inertial regime rather than the viscous one. Within the framework of two-phase models, migration can be driven by gradients of internal *normal stresses* within the particle network Σ_{ii}^p (not the total stress), and requires the fluid to filter through the granular phase to compensate for the local changes of packing fraction [20,21]. This filtration process exerts an average hydrodynamic drag $\propto U$ on the particle network, with U the average filtration velocity. The balance between these two effects controls the migration/ filtration rate, leading to $U \propto \nabla\Sigma_{ii}^p$. When injected in a mass conservation equation

$\partial\rho/\partial t = -\nabla(\rho U)$, this leads to a diffusion equation for the particle density ρ [20,21]. In the viscous regime $\Sigma_{ii}^{p} \propto \dot{\gamma}$, the timescale of migration should thus scale as $1/\dot{\gamma}$ and migration is then controlled by a (large) rate-independent strainscale, which is the classical result [19-21]. Strikingly, the same analysis performed in the inertial regime now yields an unexpected $1/\dot{\gamma}$ strainscale for migration: this explains why migration is much accelerated and abrupt when entering the inertial regime.

To confirm this analysis, we have studied the migration kinetics at constant Ω's, starting each time from a homogeneous state. Fig. 1d shows the strain needed to complete migration vs. Ω: it decreases strongly with Ω. Although the exact kinetics results from a complex history (as both $\dot{\gamma}$ and ϕ change locally in time), the asymptotic $1/\dot{\gamma}$ decay predicted by the above scaling analysis in the granular regime is roughly consistent with our observations (Fig. 1d). Migration theories based on normal stresses [20,21] are thus shown here to be more generally applicable than diffusive theories [19].

Macroscopic shear thickening — To summarize, we propose the following scenario: (i) the intrinsic behavior of dense noncolloidal suspension presents a continuous transition at low strain rates from a viscous to a shear thickening, granular, rheology characterized by shear stresses $\propto \dot{\gamma}^2$; (ii) in the granular regime, a very fast particle migration then occurs towards low shear zones; (iii) the interplay between flow and migration shows up as a sharp shear thickening of the transient macroscopic stress.

We note that our macroscopic observation (Fig. 1a) is similar to that of [7]; yet, our interpretations strongly differ. Brown and Jaeger [7] conclude that there is a transition between a viscous regime and a shear thickening regime $\tau \propto \dot{\gamma}^{1/n}$ with $n\approx0.5$ far from jamming and n continuously decreasing towards 0 upon approaching jamming. In contrast, from local observations, we claim that the intrinsic behavior of the materials shows only viscous or granular scalings (i.e. with $n=0.5$) even when $\phi \rightarrow \phi_m$, and that jamming is an abrupt transition.

To further check the robustness of the above scenario, we have studied the behavior of the same material in a parallel plate geometry. Fig. 3a shows that the macroscopic response presents strong discontinuous shear thickening. In the MRI, this transition is seen to be associated with fast shear-induced migration and to the formation of jammed regions (of volume fraction $\approx62\%>\phi_m$). We thus conclude that in general, the discontinuous shear thickening is not an intrinsic property but results from shear-induced heterogeneities in the material and originates from the intrinsic continuous shear thickening behavior.

Let us finally note that our mechanism may also be at work in Brownian suspensions, in competition with or as an alternative to hydrodynamic clustering [2]. It is compatible with the reversibility of the shear thickening transition usually observed in Brownian suspensions: migration is indeed expected to be reversible due to the osmotic pressure. It is therefore particularly striking that our mechanism leads to a constant critical shear stress, exactly what is observed for colloids [2].

We thank Daniel Lhuillier for enlightening discussions on shear-induced migration.

[1] H. A.Barnes, J. Rheol. **33**, 329 (1989).
[2] J.W. Bender, N. J. Wagner, J. Colloid Interface Sci. **172**, 171 (1995); B. J. Maranzano, N. J. Wagner, J. Chem. Phys. **117**, 10291 (2002).
[3] D. R. Foss, J. F. Brady, J. Fluid Mech. **407**, 167 (2000).
[4] J. R. Melrose, R. C. Ball, Europhys. Lett. **32**, 535 (1995); J. Rheol. **48**, 961 (2004); J. Rheol. **48**, 937 (2004); R. S. Farr *et al.*, Phys. Rev. E **55**, 7203 (1997).
[5] A. Fall *et al.,* Phys Rev Lett. **100**, 018301 (2008).
[6] E. Bertrand *et al.,* Phys. Rev. E **66**, 060401 (2002).
[7] E. Brown, H. M. Jaeger, Phys. Rev. Lett. **103**, 086001 (2009); Nature Mater. **9**, 220 (2010).
[8] Cassar *et al.*, Phys. Fluids **17**, 103301 (2005).
[9] G. Ovarlez *et al.*, J. Rheol. **50**, 259 (2006).
[10] C. Bonnoit *et al.*, J. Rheol. **54**, 65 (2010).
[11] M. E. Cates *et al.*, Phys. Rev. Lett. **81**, 1841 (1998).
[12] L. Isa *et al*, Phys. Rev. Lett. **102**, 58302 (2009).
[13] A. Fall *et al.*, Phys Rev Lett. **103**, 178301 (2009).
[14] J. F. Brady, J. F. Morris, J. Fluid Mech. **348**, 103 (1997).
[15] I.E. Zarraga *et al.*, J. Rheol. **44**, 185 (2000).
[16] D. Bonn *et al.*, Annu. Rev. Fluid Mech. **40**, 209 (2008).
[17] S. Rodts *et al.*, C. R. Chim. **7,** 275 (2004).
[18] N. Huang *et al.,* Phys. Rev. Lett. **94**, 028301 (2005).
[19] D. Leighton, A. Acrivos, J. Fluid Mech. **181**, 415 (1987); R. J. Phillips *et al.*, Phys. Fluids A **4**, 30 (1992).
[20] J. F. Morris, F. Boulay, J. Rheol. **43**, 1213 (1999).
[21] D. Lhuillier, Phys. Fluids **21**, 023302 (2009).
[22] A. Lemaître, Phys. Rev. Lett. **89**, 064303 (2002); G. Lois *et al.* Phys. Rev. E **72**, 051303 (2005).
[23] A. Lemaître *et al.*, Rheol. Acta **48**, 925 (2009).
[24] R. A. Bagnold, Proc. R. Soc. A **225**, 49 (1954).
[25] P.-E. Peyneau, PhD thesis of ENPC (2009).
[26] F. da Cruz *et al.*, Phys. Rev. E **72**, 021309 (2005).
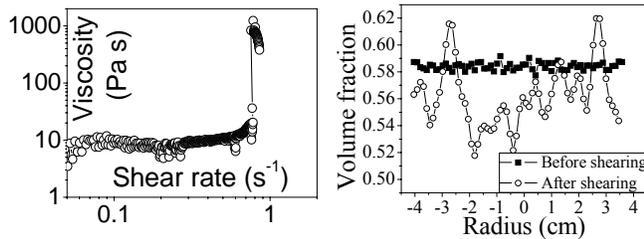[27] J.F. Brady, J. Fluid Mech. 98, 3335 (1993).

Fig. 3: a) Viscosity of a 59% suspension vs. shear rate for an increasing shear rate ramp in a 1.45mm gap parallel plate geometry. b) Volume fraction profile in a parallel plate geometry before and after shear thickening; 10cm diameter and 5mm gap were used to ensure that a signal is measured.